Available online at www.sciencedirect.com
SCIENCE DIRECT®
ELSEVIER
Journal of Environmental Radioactivity 71 (2004) 215–224
JOURNAL OF ENVIRONMENTAL RADIOACTIVITY
www.elsevier.com/locate/jenvrad

Bronchial dosimeters for radon progeny for Chinese males and females

T.T.K. Cheung, K.N. Yu *

City University of Hong Kong, Department of Physics and Materials Science, Tat Chee Avenue, Kowloon Tong, Hong Kong

Received 24 January 2003; received in revised form 28 May 2003; accepted 29 May 2003

Abstract

Bronchial dosimeters have been designed for adult Chinese males and females for home and mine exposures, which can give the bronchial doses from radon progeny by direct measurements. The bronchial dosimeter for home exposures consists of five 400-mesh wire screens. With a sampling face velocity of 3.3 cm s^{-1} for Chinese males and 2.7 cm s^{-1} for Chinese females, the deposition pattern on the wire screens were found to satisfactorily match the variation of the dose conversion coefficients (in units of mSv WLM^{-1}) with the size of radon progeny from 1 to 1000 nm. The bronchial dosimeter for mine exposures consists of four 250-mesh wire screens. With a sampling face velocity of 3.3 cm s^{-1}, the deposition pattern on the wire screens were found to satisfactorily match the variation of the dose conversion coefficients for both Chinese males and females. In this way, the bronchial dosimeters directly give the bronchial doses from the alpha counts recorded on the wire-screens.

Keywords: Dosimetry; Dose; Lung model; Radiation

1. Introduction

Inhalation of airborne short-lived radon progeny in the indoor and outdoor environment yields the greatest amount of natural radiation exposure to the public. To assess the corresponding bronchial dose, the use of dosimetric lung models is necessary. As such, it is of interest to find ways to measure the bronchial dose

* Corresponding author. Tel.: +1-852-2788-7812; fax: +1-852-2788-7830.
E-mail address: peter.yu@cityu.edu.hk (K.N. Yu).

0265-931X/$ - see front matter © 2003 Elsevier Ltd. All rights reserved.
doi:10.1016/S0265-931X(03)00170-X

directly. Based on the collection efficiencies of wire screens, Cheung et al. (2001) outlined the conceptual procedures for developing a dosimeter for the ICRP model for typical home and mine conditions. Following the radon progeny dosimetric modeling for Chinese males and females (Yu et al., 2001), the present work extends the study to the design of dosimeters for Chinese males and females, for typical home and mine conditions.

2. Methodology

2.1. Dosimetric lung model

In the present work the ICRP lung morphometry model (ICRP, 1994) has been employed. Effects of different lung morphometry models on the calculated dose conversion coefficient (DCC) from radon progeny have been studied previously (Nikezic et al., 2000). The tracheobronchial (T-B) tree is considered to comprise bronchial (BB) and bronchiolar (bb) regions. The nuclei of secretory and basal cells have been considered to be the sensitive targets in the BB region while only secretory cells have been considered in the bb region. Equal radio-sensitivities were assumed for these two types of cells. Radiation doses to tissues and cells of the respiratory tract are functions of the air flow rate through the lung passages. To predict radiation doses for different types of population groups, different breathing rates need to be matched to particular situations. Reference values of breathing rates for mine workers (mines) and members of the public (homes) have been chosen to be 1.2 $m^3\ h^{-1}$ and 0.78 $m^3\ h^{-1}$, respectively (Zock et al., 1996).

Estimate of the fractions of inhaled progeny deposited in each anatomical region is the next step in this process. Several processes contribute to the aerosol deposition. The most important of the mechanisms include Brownian diffusion, inertial impaction and sedimentation. To provide a straightforward model, an empirical mathematical approach was applied to describe the regional deposition in the extrathoracic and thoracic airways (ICRP, 1994; James et al., 1991; NRC, 1991). It is noted that the difference between the DCCs obtained using different existing formulae can be as high as 30% (Nikezic et al., 2002). The deposited progeny are assumed to distribute uniformly on the surfaces, and are cleared by mucociliary transport or absorption into blood with an assumed transit time of 10 h for the slow transfer process (Zock et al., 1996).

To sum the regional doses for the respiratory tract, they must be adjusted for their relative radiation sensitivities. The total lung dose was calculated by introducing the same weighted apportionment factor of 0.333 for BB and bb. The tissue weighting factor of 0.12 specified for lungs was also applied to the total dose calculated for the thoracic region, together with the radiation weighting factor of 20 for alpha particles, to obtain the effective dose. Dividing by the exposure, the dose conversion coefficient (DCC) in unit of mSv WLM^{-1} was obtained.

2.2. Scaling for Chinese males and females

In the present work, the ethnic groups of Chinese males and the Chinese females are considered. Scaling can make use of information on parameters such as the functional residual capacity (FRC), weight, the total lung capacity (TLC), and the vital capacity (VC) (Yu et al., 2001). The values of these parameters for Caucasian adult males as compared with those for the Chinese males and females have been summarized by Roy et al. (1991). Two different scaling factors are employed; one for linear dimension while the other for the breathing rate. For the linear scaling factor, it is taken as the average of the ratios of the FRC and the weight: the dimensions of the Caucasian lung airways are scaled with 0.95 to give those values for the Chinese males, while the dimensions of Chinese males have to be multiplied by 0.93 to give those for the Chinese females (Yu et al., 2001). In calculating the scaling factor for the breathing rates, the ratios of TLC, FRC and VC are taken into account: the breathing rate of Caucasian males is scaled by 0.81 to get the rate for Chinese males, while the breathing rate for Chinese females is equal to 0.71 that for the Chinese males (Yu et al., 2001).

2.3. Fitting the NDF distribution

Based on the definition of an occupational working month as 170 h and making provision for an occupancy factor, a factor for effective dose rate (EDF) having the units of mSv $(\text{s.WL})^{-1}$ or mSv $(\text{y.WL})^{-1}$ could be derived from the DCC. The EDF distribution was then normalized using a normalizing factor (n-factor) to obtain the distribution of normalized effective dose rate (NDF). In other words, the NDF curve will have a maximum value of unity. The task is then to find a system of wire screens, together with a corresponding sampling face velocity, which has a collection efficiency curve matching the NDF curve. The PAEC collected by this system, when multiplied by the n-factor, will then give the bronchial dose rate.

Based on the fan model filtration theory (Cheng and Yeh, 1980; Cheng et al., 1980), a semi-empirical equation of particle penetration through wire screens was employed. The penetration for a wire screen, with solid volume fraction α, wire thickness w and diameter d_f, is given by

$$P = \exp\left(-\frac{4\alpha w}{\pi(1-\alpha)d_f}\varepsilon\right) \tag{1}$$

where ϵ is the single fiber collection efficiency expressed as a sum of the efficiencies for several deposition processes including diffusion ϵ_{d}, interception ϵ_{in}, impaction ϵ_{im}, and diffusional interception ϵ_{id}. In fact, the diffusion process dominates the overall collection efficiency for particle diameters below 100 nm. The interception and impaction processes become significant after a few μm. The efficiency for diffusional interception is insignificant compared to that for diffusion for particle diameters up to beyond 1 μm. The mathematical representations for the four deposition efficiencies can be found elsewhere (Porstendörfer, 1996). The wire screen collection efficiency

is simply equal to (1−P). Using N identical wire screens in series, the exponent in Eq. (1) should be multiplied by N to obtain the gross penetration.

All of the collection efficiencies, with the exception of that for interception, change according to sampling face velocity U. Hence, the NDF curve can be changed by varying U or by using different combinations of wire screens (Cheung et al., 2001). For large particle sizes ranging from around tens of nm to 1 μm, corresponding to the attached mode of radon progeny, both techniques have failed to produce satisfactory fits to the NDF response. A k-factor, employing the residual efficiency of a filter paper for collecting radon progeny after their passing through the combination of wire screens, was introduced to compensate for the discrepancies (Cheung et al., 2001). Denoting the collection efficiencies for a combination of wire screens as ϵ_{wire}, the overall collection efficiency for the sampling system ϵ_{system} is expressed as

$$\varepsilon_{\text{system}} = \varepsilon_{wire} - k(1-\varepsilon_{wire}) \tag{2}$$

where k is the k-factor mentioned before.

2.4. Bronchial dosimeter

It is now possible to design a sampling system that can measure airborne radioactivity from which the bronchial dose rate can be determined. The schematic diagram of such a sampler is shown in Fig. 1. It consists of two sampling heads, A and B. The sample head A houses only one filter paper and collects all radon progeny passing through it. Sample head B houses a series of stainless steel wire screens on top of a filter paper. The combination of the screen series is chosen according to the purposes (for Chinese male or female, and for the mine or home environment). For example, five 400-mesh wire screens with a sampling face velocity of 3.3 cm s^{-1} has been selected to simulate the NDF distribution curve for domestic exposures for Chinese males. The collected activities on both filter papers are measured using either gross alpha or alpha spectroscopic systems. Details of the required measure-

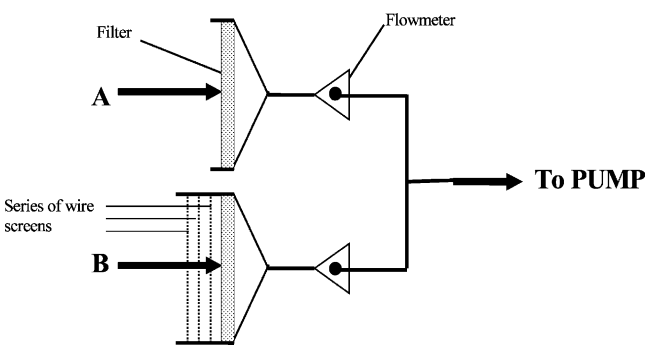

Fig. 1. Schematic diagram of the sampling system of the proposed radon progeny bronchial dosimeter. Two sampling heads are included. The choice of the wire-screen configuration in head B depends on the purpose.

ment techniques have been presented elsewhere (Yu et al., 1998). The collection efficiency of the wire screen series ϵ_{wire} is obtained by

$$\varepsilon_{wire} = \frac{PAEC_A - PAEC_B}{PAEC_A} \tag{3}$$

where $PAEC_A$ and $PAEC_B$ are the measured *PAEC*s collected on the filter papers in the sampling heads A and B, respectively. By using Eq. (2), the collection efficiency for the proposed system ϵ_{system} can be determined based on ϵ_{wire} and a selected value of *k*. The *PAEC* collected by the proposed system is computed by the product of ϵ_{system} and $PAEC_A$. This is an integral count which effectively considers size distribution over the entire size range.

3. Results and discussion

The NDF distributions for home and mine exposures for Chinese males are shown in Fig. 2. It can be observed that they have a similar pattern but very different n-factors. A higher breathing rate leads to an increase in the deposition of radon progeny and thus the dose received. Therefore, the values of DCF calculated for mine conditions referring to a larger breathing rate are always greater than those for home conditions. The maximum value of NDF is shifted to a somewhat lower particle diameter in case of mine exposures. The difference between the resulting doses mainly comes from the assigned breathing rates for these two exposure conditions.

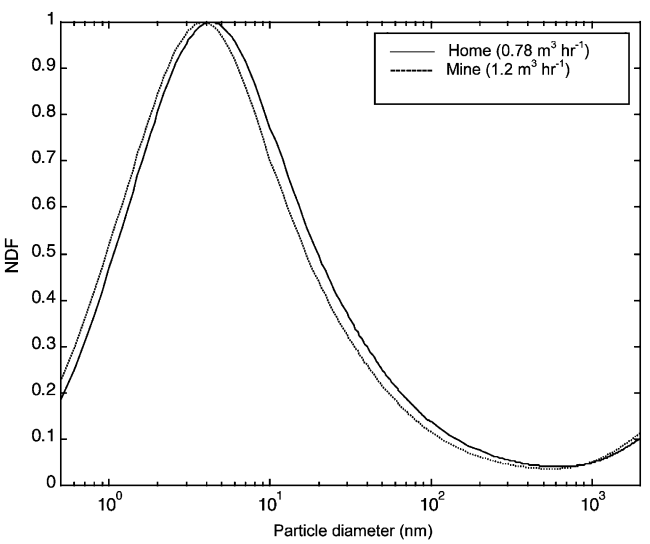

Fig. 2. The NDF as a function of particle diameter for home and mine exposures for Chinese males. The n-factors are 1.3505×10^{-4} mSv(s.WL)$^{-1}$ and 1.9502×10^{-4} mSv(s.WL)$^{-1}$, respectively. The breathing rates of 0.78 m^3 h^{-1} and 1.2 m^3 h^{-1} for home and mine exposures, respectively, apply to Caucasian males only. For the present calculations for Chinese males, the breathing rates have been scaled by 0.81.

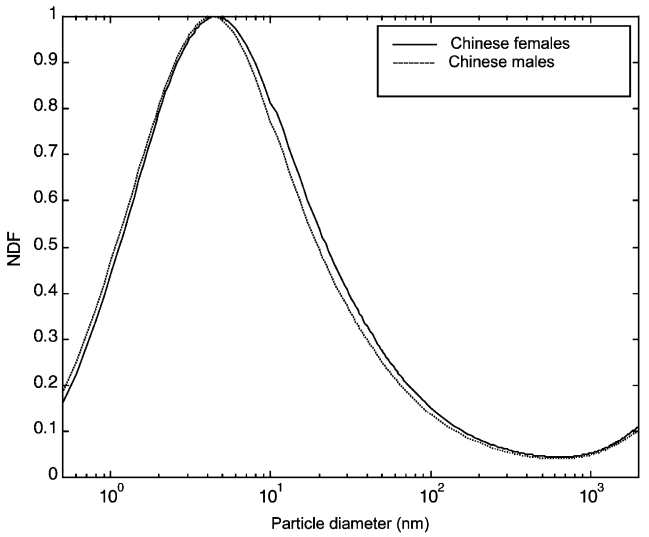

Fig. 3. The NDF distribution for Chinese females as compared to that for Chinese males (for home exposure). The n-factor for Chinese females is 1.1252×10^{-4} mSv(s.WL)$^{-1}$.

The Chinese males and females differ in the lung dimensions and the breathing rate. As an example, the NDF distribution for Chinese males and females for home exposure has been shown in Fig. 3. It can be seen that the NDF distribution for Chinese females shifts to the right as compared with that for Chinese males. The n-factor is smaller than that for Chinese males because the breathing rates for Chinese females are scaled down by 0.71 from those of the Chinese males.

Two different types, categorized by the mesh numbers, of wire screens are employed. Both types of them are made of stainless steel with a specific density of 7.8 g cm^{-3}, and the other measured parameters are summarized in Table 1. Different types or different number of wire screens combined in series change the collection efficiency of the wire screen system. On the other hand, different sampling face velocities, or flow rates can also achieve the same task. Since the sampled volume of air is a key factor affecting the final counting statistics, the sampling flow rate should be large enough to minimize errors from the counting. A practical flow rate is assumed for the simulation of the NDF distribution. The flow rate taken ranges

Table 1
Summary of the measured parameters for the wire screens employed

Mesh number	Screen diameter (cm)	Mass of screen (g)	Screen thickness (μm)	Wire diameter (μm)
250	4	0.2328	87.5	37
400	4	0.1929	57	27.5

between 2 l min^{-1} and 4 l min^{-1}, which correspond to the range of sampling face velocities between 2.7 and 5.3 cm s^{-1}. In general, an increase in the flow rate leads to a shift of the collection efficiency as a whole towards smaller particle diameters, which is caused by the decrease in the diffusional deposition of radon progeny on to the wire screen at a larger sampling flow rate. Various configurations incorporating multiple wire screens in series are then attempted to fit the variation of NDF for each sampling flow rates. In reality, various configurations with their corresponding sampling face velocities can provide similar collection efficiencies on fitting the same NDF response curve.

Table 2 reports the suggested configurations of wire-screen series with various sampling face velocities to simulate the NDF distributions obtained for home and mine exposures, respectively, for Chinese males. For home exposures, the collection efficiency of a five 400-mesh wire-screen series at a sampling face velocity of 3.3 cm s^{-1} provides the best fit to the NDF distribution. Close matches can also be achieved by other configurations of wire-screen series. In case of mine exposures, combinations of four 250-mesh or four 400-mesh wire screens with a sampling face velocity of 3.3 cm s^{-1} are capable of providing adequate fits to the NDF distribution.

The corresponding wire-screen combinations are also determined for Chinese

Table 2
Summary of possible wire-screen systems providing good fits to the predicted NDF distribution for Chinese males

Exposure condition	Wire-screen system	Sampling face velocity (cm s^{-1})	k-factor	Estimated error to dose from the attached mode (bracketed values are error estimates without taking the *k*-factor into account)
Domestic homes	4 × 400 mesh	5.3	0.015	−9.63% (−19.61%)
	4 × 400 mesh	4.6	0.010	−8.49% (−15.09%)
	5 × 250 mesh	4.6	0.027	−8.61% (−26.76%)
	4 × 400 mesh	4.0	0.006	−6.34% (−10.28%)
	5 × 250 mesh	4.0	0.023	−7.35% (−22.72%)
	5 × 400 mesh	3.3	−0.015	3.04% (12.54%)
	3 × 400 mesh	3.3	0.016	−8.69% (−19.33%)
	5 × 250 mesh	3.3	0.018	−4.69% (−16.61%)
	3 × 400 mesh	2.7	0.011	−5.45% (−12.69%)
	4 × 250 mesh	2.7	0.023	−6.00% (−21.34%)
Mine	4 × 400 mesh	5.3	0.005	−7.46% (−13.28%)
	3 × 400 mesh	4.6	0.016	−8.56% (−27.42%)
	3 × 400 mesh	4.0	0.013	−6.66% (−21.91%)
	4 × 250 mesh	3.3	0.020	−2.78% (−26.34%)
	4 × 400 mesh	3.3	-0.007	3.12% (11.11%)
	3 × 400 mesh	3.3	0.008	−4.24% (−13.56%)
	3 × 250 mesh	2.7	0.026	−5.02% (−35.89%)

Negative values in the estimated error represent underestimation while positive values represent overestimation. The wire parameters for the wire screens employed can be found in Table 1.

females as illustrated in Table 3. For home exposures, the collection efficiency of a five 400-mesh wire-screen series at a sampling face velocity of 2.7 cm s^{-1} provides the best fit to the NDF distribution. In case of mine exposures, a combination of five 400-mesh wire screens with a sampling face velocity of 4.0 cm s^{-1} provides the best fits to the NDF distribution. The second best fit is achieved by a combination of four 250-mesh wire screens with a sampling face velocity of 3.3 cm s^{-1}.

As mentioned in Section 2.3, a *k*-factor is introduced to improve the agreement between the collection efficiencies and the NDF distribution for the attached mode. An example of such an improvement is presented in Fig. 4 employing a five 250-mesh wire-screen series at a sampling face velocity of 3.3 cm s^{-1} for Chinese males for home exposures, where the estimated error of the dose from the attached mode is about 17% before modification by the *k*-factor. On introducing a *k*-factor of 0.018, the error of the dose from the attached mode becomes less than 5%. All estimated errors of possible wire screen combinations are presented in Tables 2 and 3.

The collection efficiencies of all wire-screen series are always equal to unity for particle sizes below 3 nm, which have overestimated the NDF distribution in this particle-size range. In a previous study (Cheung et al., 2001), an f-factor was introduced to account for the discrepancy, for which an additional single 100-mesh wire screen was involved. However, since the unattached fractions of PAEC are only 8 and 1% in homes and mines, the errors in the dose calculations introduced by the discrepancies within this region will only be minimal, if not negligible. Therefore,

Table 3
Summary of possible wire-screen systems providing good fits to the predicted NDF distribution for Chinese females

Exposure condition	Wire-screen system	Sampling face velocity (cm s^{-1})	k-factor	Estimated error to dose from the attached mode (bracketed values are error estimates without taking the *k*-factor into account)
Domestic homes	5 × 400 mesh	5.3	0.008	−8.85% (−13.76%)
	4 × 400 mesh	4.0	0.013	−8.52% (−16.54%)
	4 × 400 mesh	3.3	0.006	−6.06% (−9.72%)
	5 × 250 mesh	3.3	0.024	−7.55% (−22.49%)
	5 × 400 mesh	2.7	-0.016	4.94% (14.31%)
	3 × 400 mesh	2.7	0.017	−8.28% (−18.80%)
Mine	5 × 250 mesh	4.6	0.023	−6.76% (−31.64%)
	5 × 400 mesh	4.0	-0.011	0.51% (11.93%)
	3 × 400 mesh	4.0	0.018	−8.99% (−28.40%)
	4 × 250 mesh	3.3	0.024	−6.48% (−32.47%)
	3 × 400 mesh	3.3	0.013	−6.80% (−20.72%)
	3 × 250 mesh	2.7	0.031	−7.41% (−41.25%)

Negative values in the estimated error represent underestimation while positive values represent overestimation. The wire parameters for the wire screens employed can be found in Table 1.

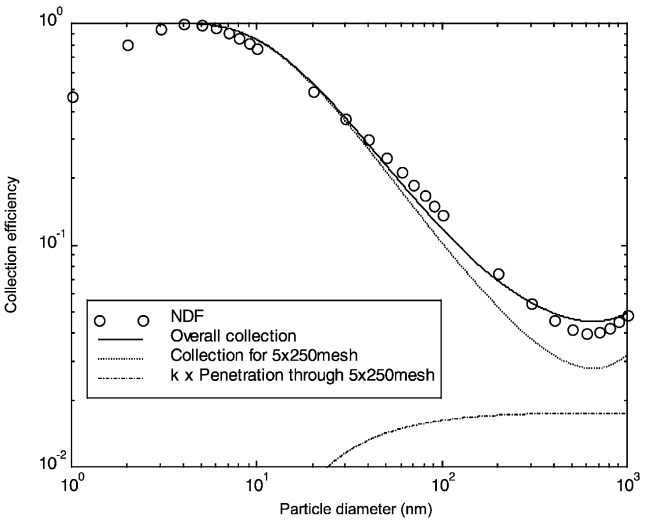

Fig. 4. The overall collection efficiency of a five 250-mesh wire-screen series plus the additional contribution from the *k*-factor. The sampling face velocity is 3.3 cm s^{-1} and the *k*-factor is 0.018. The NDF distribution is calculated for Chinese males for home exposures.

in order to save the effort of measuring an extra 100-mesh wire screen, the f-factor will not be introduced in the present study.

4. Conclusions

The designs of bronchial dosimeters which directly give the bronchial dose from radon progeny for Chinese males and female for home and mine exposures have been given in this paper. The prime advantage of these dosimeters is that no requirement exists for measurement of the size distribution of radon progeny. The particle size dependence of the NDF, which is normalized from the dose conversion coefficient, can be simulated by the collection efficiency of the proposed wire-screen sampling systems. The *k*-factor has been used as a fine-tuning technique to minimize discrepancies in the particle size region corresponding to the attached mode of radon progeny.

Various combinations of wire-screens in series have been found capable of providing satisfactory fits to the NDF pattern. For home exposures, the collection efficiency of a five 400-mesh wire-screen series provides the best fits to the NDF distributions for Chinese males and females, at sampling face velocities of 3.3 and 2.7 cm s^{-1}, respectively. This indicates that the same bronchial dosimeter can be used for measuring bronchial doses for Chinese males and females, requiring only adjustment of the flow rate and the use of different *k*-factors for the two groups. For mine exposures, the collection efficiency of a four 250-mesh wire screens with a sampling face velocity of 3.3 cm s^{-1} provides the best fit to the NDF distributions for Chinese

males and the second best fit to the NDF distributions for Chinese females. This provides even more convenience than in the home exposure condition since the same bronchial dosimeter with the same flow rate can be used for measuring bronchial doses for Chinese males and females, with the use of different *k*-factors for the two groups.

Acknowledgements

This research was supported by a research grant 7001101 from the City University of Hong Kong.

References

Cheng, A.Y.S., Yeh, H.C., 1980. Theory of screen type diffusion battery. J Aerosol Sci 11, 313–319.

Cheng, A.Y.S., Keating, J.A., Kanapilly, G.M., 1980. Theory and calibration of a screen-type diffusion battery. J Aerosol Sci 11, 549–556.

Cheung, T.T.K., Yu, K.N., Nikezic, D., 2001. Bronchial dosimeter for radon progeny. Appl Radiat Isotop 55, 707–713.

ICRP, 1994. International Commission on Radiological Protection, Human Respiratory Tract Model for Radiological Protection. Pergamon, Oxford.

James, A.C., Stahlhofen, W., Rudolf, G., Egan, M.J., Nixon, W., Gehr, P., Briant, J.K., 1991. The respiratory tract deposition model proposed by the ICRP Task Group. Radiat Prot Dosim 38, 159–165.

Nikezic, D., Yu, K.N., Cheung, T.T.K., Haque, A.K.M.M., Vucic, D., 2000. Effects of different lung morphometry models on the calculated dose conversion factor from Rn progeny. J Environ Radioac 47, 263–277.

Nikezic, D., Haque, A.K.M.M., Yu, K.N., 2002. Effects of different deposition models on the calculated dose conversion factors from ^{222}Rn progeny. J Environ Radioac 61, 305–318.

NRC, 1991. Comparative dosimetry of radon in mines and homes. Panel on Dosimetric Assumption Affecting the Application of Radon Risk Estimates. National Research Council. National Accademy Press. Washington, DC.

Porstendörfer, J., 1996. Radon: Measurements related to dose. Environ Internat 22 (Suppl. 1), S563–S583.

Roy, M., Becquemin, M.H., Bouchikin, A., 1991. Ventilation rates and lung volumes for lung modelling purposes in ethnic groups. Radiat Prot Dosim 38, 49–55.

Yu, K.N., Guan, Z.J., Young, E.C.M., Stokes, M.J., 1998. Measurement of tracheobronchial dose from simultaneous exposure to environmental radon and thoron progenies. Health Physics 75, 153–158.

Yu, K.N., Cheung, T.T.K., Haque, A.K.M.M., Nikezic, D., Lau, B.M.F., Vucic, D., 2001. Radon progeny dose conversion coefficients for chinese males and females. J Environ Radioac 56, 327–340.

Zock, C., Porstendörfer, J., Reineking, A., 1996. The influence of biological and aerosol parameters of inhaled short-lived radon decay products on human lung dose. Radiat Prot Dosim 63, 197–206.